




Cite this: *Phys. Chem. Chem. Phys.*,  
2017, **19**, 26527

Received 14th July 2017,  
Accepted 3rd August 2017

DOI: 10.1039/c7cp04762b

rsc.li/pccp

# Isotope effects on the resonance interactions and vibrational quantum dynamics of fluoroform $^{12,13}\text{CHF}_3^\dagger$

Sieghard Albert,<sup>a</sup> Elena Bekhtereva,<sup>ab</sup> Irina Bolotova,<sup>a</sup> Ziqiu Chen,<sup>a</sup> Csaba Fábri,<sup>a</sup>  
Hans Hollenstein,<sup>a</sup> Martin Quack <sup>\*a</sup> and Oleg Ulenikov<sup>ab</sup>

We report a comparison of the analysis of the low energy spectrum of  $^{13}\text{CHF}_3$  and  $^{12}\text{CHF}_3$  from the THz (FIR) range to the  $\nu_1$  fundamental at high resolution ( $\delta\tilde{\nu} < 0.001 \text{ cm}^{-1}$  or otherwise Doppler limited) on the basis of FTIR spectra taken both with ordinary light sources and with the synchrotron radiation from the Swiss Light Source. Several vibrational levels are accurately determined including, in particular, the  $2\nu_4$  CH-bending overtone and the  $\nu_1$  CH-stretching fundamental of  $^{13}\text{CHF}_3$ . Comparison of experimental results with those from accurate full dimensional vibrational calculations allows for a study of the time-dependent quantum dynamics of intramolecular vibrational redistribution (IVR) in the CH chromophore both on short time scales (fs) and longer time scales (ps) when coupling to the lower frequency modes becomes important and where the  $^{12}\text{C}/^{13}\text{C}$  isotope effects are very large.

## 1 Introduction

Fluoroform (trifluoromethane,  $\text{CHF}_3$ ) has been a prototype molecule for the study of intramolecular vibrational redistribution (IVR) and energy flow for a long time (see the reviews ref. 1, 2 and references cited therein). While the pronounced Fermi resonance polyad structure in the overtone spectra of the CH chromophore, arising from the strong interaction between the CH stretching and bending vibrations has been well analysed and understood for both  $^{12}\text{CHF}_3$ <sup>3–6</sup> and  $^{13}\text{CHF}_3$ ,<sup>7</sup> the high resolution spectrum of the  $\nu_1$  fundamental of  $^{12}\text{CHF}_3$  shows a very complex structure due to interactions with the lower frequency modes, which has resisted so far a complete analysis in spite of repeated attempts.<sup>3,8–10</sup> One possibility to approach the problem of IVR in  $\text{CHF}_3$  on longer time scales is to complete a high resolution analysis of the  $\nu_1$

fundamental in the isotopomer  $^{13}\text{CHF}_3$ , where the spectrum is greatly simplified<sup>7</sup> and transfer the corresponding knowledge by the aid of full-dimensional vibrational quantum dynamics theory<sup>11</sup> also to the other isotopomer. Such an analysis has become possible because of the more recent availability of rather accurate full-dimensional potential hypersurfaces<sup>12–16</sup> one of which will be shown to be of sufficient accuracy in comparison with experiment on the two isotopomers in order to be useful for quantum dynamics at near to spectroscopic accuracy.

The isotopomers of  $\text{CHF}_3$  are of interest in several contexts. The second most abundant isotopomer  $^{13}\text{CHF}_3$  with about 1% natural abundance is important in atmospheric spectroscopy. This isotopomer has also been studied in the context of infrared multiphoton excitation and  $^{13}\text{C}$  laser isotope separation.<sup>17–20</sup> In particular the isotopically selective intermolecular vibrational energy transfer was studied experimentally.<sup>21,22</sup> Isotope effects are also important in the context of intramolecular dynamics and intramolecular vibrational energy redistribution (IVR).

The deuterium isotope effect on the spectra and dynamics in  $\text{CDF}_3$  is obviously very large.<sup>23,24</sup> Of particular relevance for the present work is, however, the detailed investigation of the much smaller isotope effect on IVR in  $^{13}\text{CHF}_3$ .<sup>2,7,25</sup> In this case the modest change in mass leads to an only modest effect on the strong CH-stretching CH-bending Fermi resonance polyads, whereas the much weaker further resonances coupling the CH-chromophore to the heavy atom frame are changed very substantially. Hollenstein *et al.*<sup>7</sup> had obtained rather complete IR spectra for  $^{13}\text{CHF}_3$  at in part high resolution, but a detailed analysis was carried out only for the CH-stretching–bending Fermi resonance polyads with  $N = 1, 2, 3, 4$  (covering the spectral ranges up to about  $12000 \text{ cm}^{-1}$ ). The  $4\nu_1$  band in the  $N = 4$  polyad was later also studied again in ref. 26. It is the aim of the present work to investigate the  $^{13}\text{C}$  isotope effect in the lower frequency spectra of  $^{13}\text{CHF}_3$  from the far infrared ( $25 \text{ cm}^{-1}$ ) to the range of the CH-stretching fundamental  $\nu_1$  near  $3000 \text{ cm}^{-1}$  at very high resolution. In particular, we shall show that the spectrum of the  $\nu_1$  fundamental is simplified considerably for the  $^{13}\text{CHF}_3$  isotopomer allowing for a

<sup>a</sup> Physical Chemistry, ETH-Zürich, CH-8093, Zürich, Switzerland.

E-mail: martin@quack.ch; Fax: +41-44-632-1021; Tel: +41-44-632-4421

<sup>b</sup> Institute of Physics and Technology, National Research Tomsk Polytechnic University, Tomsk 634050, Russia

† Electronic supplementary information (ESI) available: Linelists of transitions assigned are included. See DOI: 10.1039/c7cp04762b

straightforward high resolution analysis of this fundamental in contrast to  $^{12}\text{CHF}_3$ .

A comparison of the spectroscopic analysis with an accurate nine-dimensional vibrational eigenstate calculation on accurate potential hypersurfaces allows us then to provide a preliminary analysis of the fully nine-dimensional time-dependent quantum dynamics including the  $^{13}\text{C}$  isotope effect on the resonance couplings to the lower frequency modes. Our results are in part based on ref. 27 (see also ref. 28).

## 2 Experimental

The synthesis of  $^{13}\text{CHF}_3$  was performed by Daniel Zindel in our laboratory at ETH Zürich, following the previously used scheme of ref. 7, 20 and 29 with some improvements as described in ref. 28. The identity and purity of the sample of  $^{13}\text{CHF}_3$  was confirmed with gas chromatography coupled with mass spectrometry, and was also obvious from the high resolution infrared spectra.

A high-resolution FTIR spectrum of  $^{13}\text{CHF}_3$  was measured at  $T = 296\text{ K}$ , using the Bruker IFS 125 HR Zurich Prototype 2001 (ZP2001) spectrometer.<sup>30,31</sup> A White-type multireflection cell with an absorption path length of 3.2 m was filled with 0.15 mbar of  $^{13}\text{C}$ -fluoroform to exclude pressure broadening. An aperture of 0.8 mm and typically a nominal resolution defined<sup>31</sup> as  $\delta\tilde{\nu} = 1/d_{\text{MOPD}}$  of  $0.0015\text{ cm}^{-1}$  were used to provide essentially Doppler limited spectra in the range  $2600\text{--}3100\text{ cm}^{-1}$  ( $\Delta\tilde{\nu}_D \approx 0.004\text{ cm}^{-1}$ ). A total of 200 scans were co-added to increase the signal-to-noise ratio. A global light source, a  $\text{CaF}_2$  beamsplitter and an InSb detector were used in these experiments. Fig. 1 shows as an example a survey of the  $2\nu_4$  spectral range for  $^{13}\text{CHF}_3$  as compared to  $^{12}\text{CHF}_3$ , and Fig. 2 shows a similar overview for the  $\nu_1$  range. Spectra in the range 25 to  $1500\text{ cm}^{-1}$  have been reported and analysed in ref. 28.

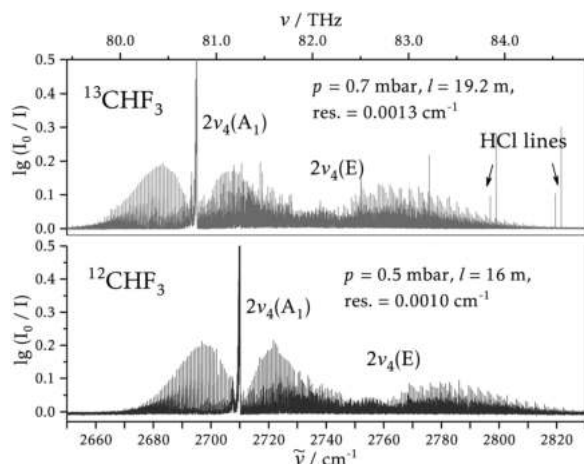


Fig. 1 Survey of the  $2\nu_4(A_1/E)$  band of  $^{13}\text{CHF}_3$  measured at 296 K with a nominal resolution  $\delta\tilde{\nu} = 0.0013\text{ cm}^{-1}$  (upper trace) compared to the spectrum of  $^{12}\text{CHF}_3$ ,  $\delta\tilde{\nu} = 0.0010\text{ cm}^{-1}$ , (lower trace). The  $A_1$  component of the band has a pronounced Q-branch, from which an isotopic shift of about  $15\text{ cm}^{-1}$  can be observed. Absorbance is shown as decadic logarithm,  $\lg(I_0/I)$ .

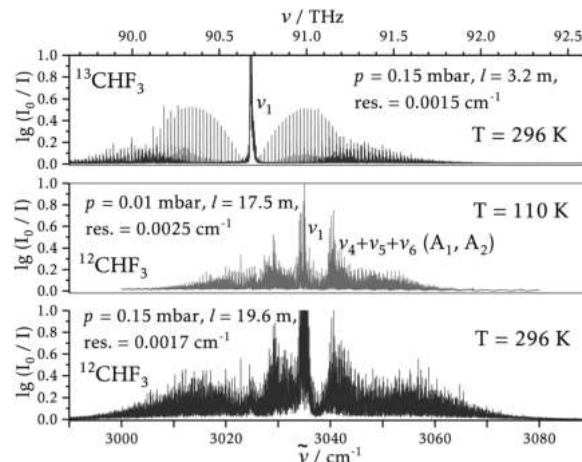


Fig. 2 Survey of the  $\nu_1$  fundamental band of  $^{13}\text{CHF}_3$  measured at  $p = 0.15\text{ mbar}$ ,  $l = 3.2\text{ m}$ ,  $\delta\tilde{\nu} = 0.0015\text{ cm}^{-1}$  ( $\Delta\tilde{\nu}_D = 0.0044\text{ cm}^{-1}$  at  $\tilde{\nu}_0 = 3030\text{ cm}^{-1}$ ) and  $T = 296\text{ K}$  (top) and of the corresponding band of  $^{12}\text{CHF}_3$  measured with nominal resolutions ( $\delta\tilde{\nu}$ ) of  $0.0025\text{ cm}^{-1}$  and  $0.0017\text{ cm}^{-1}$  respectively (middle and bottom, at  $\tilde{\nu} = 3030\text{ cm}^{-1}$   $^{12}\text{CHF}_3$  has  $\Delta\tilde{\nu}_D = 0.0044\text{ cm}^{-1}$  at  $T = 296\text{ K}$  and  $\Delta\tilde{\nu}_D = 0.0027\text{ cm}^{-1}$  at  $T = 110\text{ K}$ ). Only  $\nu_1$  of  $^{13}\text{CHF}_3$  shows the simple structure typical for the  $A_1$ -symmetry bands of fluoroform. Absorbance is shown as decadic logarithm,  $\lg(I_0/I)$ .

## 3 Theoretical model

The theoretical model Hamiltonian for the analysis of the spectra was used here in the form derived in ref. 32–35 (see also ref. 63). We describe it here briefly in order to provide a definition of spectroscopic parameters reported below. For effectively isolated vibrational states of  $A_1$  symmetry we have only used a diagonal block for unperturbed vibrational states in the following form:

$$\begin{aligned} \hat{H}^{A_1 A_1}/(\text{hc}) = & |A_1\rangle\langle A_1| \{ E^a + B^a(\hat{J}_x^2 + \hat{J}_y^2) + C^a \hat{J}_z^2 \\ & - D_J^a \hat{J}^4 - D_{JK}^a \hat{J}^2 \hat{J}_z^2 - D_K^a \hat{J}_z^4 \\ & + H_J^a \hat{J}^6 + H_{JK}^a \hat{J}^4 \hat{J}_z^2 + H_{KJ}^a \hat{J}^2 \hat{J}_z^4 + H_K^a \hat{J}_z^6 \\ & + L_J^a \hat{J}^8 + L_{JK}^a \hat{J}^6 \hat{J}_z^2 + \dots \} \end{aligned} \quad (1)$$

$E^a(\text{hc})$  is the unperturbed vibrational energy of the level of  $A_1$  symmetry and the rotational parameters  $B^a$ ,  $C^a$  etc. have their usual meaning, see ref. 32–35. Diagonal blocks describing the states of  $E$ -symmetry arise in the following form:

$$\begin{aligned} \hat{H}^{EE}/(\text{hc}) = & (|E_1\rangle\langle E_1| + |E_2\rangle\langle E_2|) \\ & \{ E^c + B^c(\hat{J}_x^2 + \hat{J}_y^2) + C^c \hat{J}_z^2 \\ & - D_J^c \hat{J}^4 - D_{JK}^c \hat{J}^2 \hat{J}_z^2 - D_K^c \hat{J}_z^4 + H_J^c \hat{J}^6 \\ & + H_{JK}^c \hat{J}^4 \hat{J}_z^2 + H_{KJ}^c \hat{J}^2 \hat{J}_z^4 + H_K^c \hat{J}_z^6 \\ & + L_J^c \hat{J}^8 + L_{JK}^c \hat{J}^6 \hat{J}_z^2 + \dots \} \\ & + (|E_1\rangle\langle E_2| - |E_2\rangle\langle E_1|) \{ \eta^{vE} \hat{J}_z + \eta_J \hat{J}_z \hat{J}^2 + \dots \} \end{aligned} \quad (2)$$

Off-diagonal blocks, when interactions are taken into account, are given by (with  $i = \sqrt{-1}$ ):

$$\begin{aligned} \hat{H}^{A_1 E} / (\text{hc}) = & |A_1\rangle\langle E_1| \left\{ \left[ \hat{A}, (\hat{J}_+ - \hat{J}_-) \right]_+ + \left[ \hat{B}, (\hat{J}_+ + \hat{J}_-) \right]_+ \right. \\ & + \left. \left[ \hat{C}, (\hat{J}_+^2 + \hat{J}_-^2) \right]_+ + \left[ \hat{D}, (\hat{J}_-^2 - \hat{J}_+^2) \right]_+ \right\} \\ & + |A_1\rangle\langle E_2| \left\{ \left[ \hat{A}, (\hat{J}_+ + \hat{J}_-) \right]_+ + \left[ \hat{B}, (\hat{J}_- - \hat{J}_+) \right]_+ \right. \\ & + \left. \left[ \hat{C}, (\hat{J}_+^2 - \hat{J}_-^2) \right]_+ + \left[ \hat{D}, (\hat{J}_+^2 + \hat{J}_-^2) \right]_+ \right\}. \end{aligned} \quad (3)$$

The operators  $\{\hat{A}, \hat{B}, \hat{C}, \hat{D}\}$  can be expressed as:

$$\begin{aligned} \hat{A} &= \frac{1}{2}\tilde{\alpha} + \frac{1}{2}\tilde{\alpha}_J \hat{J}^2 + \tilde{\alpha}_K \hat{J}_z^2 + \dots, \\ \hat{B} &= \tilde{\beta} \hat{J}_z + \tilde{\beta}_J \hat{J}_z \hat{J}^2 + \tilde{\beta}_K \hat{J}_z^3 + \dots, \\ \hat{C} &= \frac{1}{2}\tilde{\gamma} + \frac{1}{2}\tilde{\gamma}_J \hat{J}^2 + \tilde{\gamma}_K \hat{J}_z^2 + \dots, \\ \hat{D} &= \tilde{\delta} \hat{J}_z + \tilde{\delta}_J \hat{J}_z \hat{J}^2 + \tilde{\delta}_K \hat{J}_z^3 + \dots \end{aligned} \quad (4)$$

This model was tested and exploited to describe the FTIR spectra of  $^{12}\text{CHF}_3$ , where numerous interactions can be

found.<sup>27,28,36</sup> The effective Hamiltonian model defines the notation used in Table 1.

It should be noted that nuclear hyperfine structure and parity substructure are not resolved in our experiments thus each  $E$  level in  $C_{3v}$  has an effective weight of 8, which is a combination of nuclear spin and parity degeneracy weights.  $A_1$  and  $A_2$  levels have well-defined parity here.<sup>37,38</sup> As for  $|K| = 3n$  (integer  $n$ ) the splittings of the  $A_1$  and  $A_2$  sub-levels are not resolved in the present spectra, the effective weights for these doublets are thus 16. For more details see ref. 27, 28 and 36–38. Thereby, in the experimental spectrum one observes a relative ratio 1 : 1 : 2 of intensities for transitions with  $e : e : (a_1/a_2)$  symmetry, see Fig. 3. These effective relative weights enter in the simulation of spectra.

The selection rules for electric dipole matrix elements require approximate conservation of nuclear spin symmetry and change of parity. Therefore, the allowed transitions are given by eqn (5) and (6),<sup>37,38</sup> when the full permutation inversion group  $S_3^+$  is used (with species  $A_2^\pm, E^\pm$ , only  $A_1^\pm$  being forbidden by the Pauli principle):

$$A_2^+ \leftrightarrow A_2^- \quad (5)$$

and

$$E^+ \leftrightarrow E^- \quad (6)$$

with all other transitions being strongly forbidden by the principle of nuclear spin symmetry conservation. Further approximate

**Table 1** Spectroscopic parameters of the  $2\nu_4(A_1/E)$  vibrational state and of  $\nu_1$  for  $^{13}\text{CHF}_3$  (in  $\text{cm}^{-1}$ )<sup>a</sup>

Parameter	g.s. <sup>28</sup>	$2\nu_4(A_1)$	$2\nu_4(E)$	$\nu_1$
1	2	3	4	5
$E^{a,e}$	0.0	2695.18841(12)	2737.46695(24)	3024.6131994(299)
$\tilde{\nu}_0$	0.0	2695.18841(12)	2737.46695(24)	3024.6131994(299) <sup>e</sup>
$B$	0.344304863	0.34366245(33)	0.34366244(92)	0.3442816(463)
$C$	0.1892506 <sup>b</sup>	0.18913705(43)	0.189128(13)	0.1894430(970)
$D_J/10^{-6}$	0.373859	0.36976(20)	0.38007(69)	0.36709(135)
$D_{JK}/10^{-6}$	-0.596077	-0.58888(46)	-0.596077	-0.9906(10)
$D_{K^2}/10^{-6}$	0.3024 <sup>b</sup>	0.27394(33)	0.2779	0.29707(30)
$H_J/10^{-12}$	0.6217	0.6217	0.6217	0.6217
$H_{JK}/10^{-11}$	-0.283	-0.283	-0.283	-0.283
$H_{KJ}/10^{-11}$	0.343	0.343	0.343	0.343
$H_{K^2}/10^{-11}$	-0.1428 <sup>g</sup>	-0.1428	-0.1428	-0.1428
$L_{JK}/10^{-17}$	-0.13	-0.13	-0.13	-0.13
$L_{K^2}/10^{-16}$	0.2	0.2	0.2	0.2
$\eta$			-0.7403808(686) <sup>f</sup>	
$\eta_J/10^{-5}$			0.243(16)	
$\alpha/10^{-3}$			0.186(88)	
Interaction parameters $2\nu_4(A_1/E)$ :				
$\tilde{\alpha}_J/10^{-5}$			0.11(19)	
$J^{\text{max}}$	90	41	40	24
$K^{\text{max}}$	88	40	7	15
$N_{\text{data}}$	85 + 3487 <sup>c</sup>	938	140	224
$d_{\text{rms}}$	0.00015 <sup>d</sup>		0.0011	0.00064

<sup>a</sup> Values in parentheses are  $1\sigma$  standard uncertainties. Parameters presented without uncertainties were fixed to the values of the corresponding parameters of the vibrational ground state (g.s.). <sup>b</sup> Value for the  $^{12}\text{CHF}_3$  species. The *ab initio* prediction for  $A_0 = C_0(^{12}\text{C}) - C_0(^{13}\text{C}) = -2 \times 10^{-5} \text{ cm}^{-1}$  being small. <sup>c</sup> 85 microwave transitions from ref. 42–44 were combined with 3487 Terahertz lines measured in ref. 28. The fitted transitions were weighted with the inverse of experimental uncertainty. <sup>d</sup> For the infrared transitions. <sup>e</sup> Ref. 45 provided a rough estimate of 3025.28  $\text{cm}^{-1}$  from low resolution data. Ref. 7 gave  $\tilde{\nu}_0 = 3024.6 \text{ cm}^{-1}$  at higher resolution, but without full analysis. Here  $\tilde{\nu}_0$  is the vibrational term value (with  $J = 0$ ). <sup>f</sup> The parameter  $\eta^{vE}$  can be related to the conventional  $C_J^v$  by  $\eta^{vE} = 2C_J^v$  for the fundamental and by  $\eta^{vE} = -4C_J^v$  for the overtone (see ref. 63). <sup>g</sup> The parameter  $H_K$  is fixed to the value for the ground state of  $^{12}\text{CHF}_3$  as calculated *ab initio* by G. Klatt, A. Willetts, N. C. Handy, R. Tarroni and P. Palmieri, *J. Mol. Spectrosc.*, 1996, **176**, 64–74 (see also ref. 15).

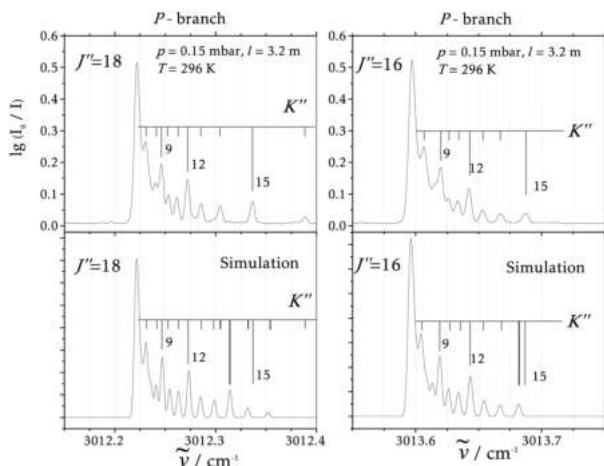


Fig. 3 Part of the P-branch of the  $\nu_1$  fundamental of  $^{13}\text{CHF}_3$  showing the clusters of rovibrational lines with  $J'' = 16$  and  $J'' = 18$  (upper boxes) compared to simulations with the parameters from the Table 1 (bottom). One can observe that due to the local perturbations the lines with  $K'' \geq 15$  are shifted in the experimental spectrum. This could be treated by taking into account a local interaction of the  $\nu_1$  fundamental with a resonance partner or else the perturbed lines are omitted in the fitting procedure. Absorbance is shown as decadic logarithm,  $\lg(I_0/I)$ .

selection rules arise in the usual way from the properties of the rovibronic wavefunctions.<sup>39,40</sup>

We have also carried out full-dimensional vibrational calculations (for the  $J = 0$  levels) using the DEWE (Discrete Variable Representation of the Eckart–Watson Hamiltonian with Exact Inclusion of an Arbitrary Potential Energy Function) program package<sup>11</sup> to obtain numerically exact vibrational energy levels and wavefunctions for  $^{12}\text{CHF}_3$  and  $^{13}\text{CHF}_3$ . We tested two different potential energy surfaces (PESs) provided by ref. 12 and 14. The more accurate PES published in ref. 14 has been selected for our theoretical quantum-dynamical investigations. Vibrational intensities were evaluated using the electric dipole moment surface (DMS) published in ref. 14. 8 Hermite DVR (discrete variable representation) basis functions were used for each vibrational degree of freedom resulting in a direct product DVR basis of dimension  $8^9 = 134\,217\,728$ .  $C_{3v}$  symmetry labels were automatically assigned to the calculated eigenstates by the symmetry-adapted Lanczos eigensolver algorithm (see also ref. 64). Atomic masses have been employed ( $m_{^{12}\text{C}} = 12.000000\text{u}$ ,  $m_{^{13}\text{C}} = 13.003355\text{u}$ ,  $m_{\text{H}} = 1.007825\text{u}$  and  $m_{^{19}\text{F}} = 18.998403\text{u}$ ) throughout this work, harmonic frequencies and normal coordinates needed for defining the Hermite DVR vibrational basis and constructing the Eckart–Watson Hamiltonian were obtained at the MP2/6-311++G(3df,2pd) level of theory (corresponding to the level of theory used in ref. 14) by the Gaussian 09 program package.<sup>41</sup>

## 4 Analysis of the spectra

The  $\nu_1$  CH-stretching fundamental of  $^{13}\text{CHF}_3$  was measured at low resolution in ref. 45 and at higher resolution in ref. 7. The band center in ref. 45 was estimated from the Q-branch at  $\tilde{\nu}_0 = 3025.28\text{ cm}^{-1}$ . Due to the low resolution this is shifted from

the true value of  $\tilde{\nu}_0$  by  $\sim 2B$ . Hollenstein *et al.*<sup>7</sup> gave a band center of  $\tilde{\nu}_0 = 3024.6\text{ cm}^{-1}$ , similar to our new results, but without full analysis at the time. Table 1 gives the results from an analysis of the  $2\nu_4(A_1)$  and  $2\nu_4(E)$  components of the CH-bending overtone as well as the  $\nu_1$  fundamental treated as effectively isolated band systems. For the  $\nu_1$  fundamental we assigned levels up to  $J^{\text{max}} = 24$  and  $K^{\text{max}} = 15$  but only those with  $J \leq 18$  were included in the fit. Indeed, for  $J > 15$  the  $K$ -structure is perturbed for  $K \geq 15$  as is shown with the example of the detail in Fig. 3, which also shows the characteristic intensity pattern. The corresponding local resonance is excluded from the present analysis aimed mostly at an accurate band center for  $\nu_1$ . Similarly in  $2\nu_4$  some perturbations were not taken into account, for instance the one with the level  $\nu_4 + 2\nu_3$  expected from a similar interaction observed for the fundamental  $\nu_4$  interacting with  $2\nu_3$ .<sup>28</sup> In this sense the rovibrational analysis is preliminary and in any case the parameters have an effective meaning in terms of the Hamiltonian used for the fit. In comparing parameters from different sources one must also note the differences arising from different definitions. This does not affect the rovibrational term values, and in particular the vibrational energies (with  $J = 0$ ) of interest here.

## 5 Discussion and conclusions on time-dependent vibrational dynamics (IVR)

Our present results for  $2\nu_4(A_1/E)$  and  $\nu_1$  for  $^{13}\text{CHF}_3$  provide a high-resolution picture of this important Fermi-resonance coupled polyad. As the resonance is “global” with a large separation of  $\nu_1$  and  $2\nu_4(A_1)$  one can derive accurate vibrational band centers and  $J = 0$  energy levels involved by an effectively isolated state rovibrational analysis as outlined in Table 1. Joining the present results with the earlier results from our high-resolution work and some lower resolution results for  $^{13}\text{CHF}_3$  one can obtain a survey of the current knowledge of the low energy spectrum up to the CH-stretching fundamental as outlined in Table 2 in comparison with  $^{12}\text{CHF}_3$ . In order to provide a further analysis of the vibrational quantum dynamics we have carried out full-dimensional vibrational eigenstate calculations for both isotopomers  $^{12}\text{CHF}_3/^{13}\text{CHF}_3$  on recent potential hypersurfaces, one of which proved to provide quite accurate results for  $^{12}\text{CHF}_3$ , see ref. 14. However, the detailed assignments in the  $\nu_1$  fundamental range remains uncertain for reasons discussed above. For  $^{13}\text{CHF}_3$  these uncertainties are essentially absent and we thus can provide a fairly global test of the accuracy of this potential hypersurface for the vibrational quantum dynamics of fluoroform in Table 2. In particular, testing the predictions with our new  $^{13}\text{CHF}_3$  isotopomer results indicates that the potential of Ramesh and Sibert<sup>14</sup> has near to spectroscopic accuracy in this energy range. The accuracy of the theoretical results for  $^{13}\text{CHF}_3$ , while not quite as good as for  $^{12}\text{CHF}_3$ , to which the potential had been adapted to some extent, is certainly sufficient to allow for a quantitative comparison of the time-dependent quantum dynamics for the two isotopomers, showing characteristic differences. It should be clear that the

Table 2 Experimental and theoretical results for selected vibrational energy levels of  $^{12}\text{CHF}_3$  and  $^{13}\text{CHF}_3$ 

Level	$\Gamma$	$^{12}\text{CHF}_3$ theor. <sup>a</sup>	$^{12}\text{CHF}_3$ theor. <sup>b</sup>	$^{12}\text{CHF}_3$ exp.	$^{13}\text{CHF}_3$ theor.	$^{13}\text{CHF}_3$ exp.	Ref.
		This work	This work	Ref. 36	This work	Ref. column 8	
1	2	3	4	5	6	7	8
$\nu_6$	$E$	507.079	507.805	507.822 <sup>c</sup>	506.785	507.0	45
$\nu_3$	$A_1$	703.589	700.094	700.09898	695.208	695.292	28
$\nu_2$	$A_1$	1141.717	1141.515	1141.4569	1116.152	1115.9	45
$\nu_5$	$E$	1176.486	1158.347	1157.3346	1132.408	1132.4	45
$\nu_3 + \nu_6$	$E$	1211.532	1209.092	1208.7708	1202.695	1202.6	45
$\nu_4$	$E$	1398.447	1377.505	1377.8472	1369.631	1369.013	28
$2\nu_3$	$A_1$	1405.902	1399.484	1399.3938	1389.729	1389.807	28
$\nu_2 + \nu_3$	$A_1$	1841.076	1839.634	1839.8 <sup>d</sup>	1809.436	1809.2	45
$\nu_3 + \nu_5$	$E$	1875.342	1853.367	1851.9 <sup>d</sup>	1822.926	1822	45
$\nu_2 + \nu_4$	$E$	2543.192	2518.980	2517.9 <sup>d</sup>	2485.644	2480	45
$\nu_4 + \nu_5$	$E$	2567.511	2532.624		2498.444	2489	45
$2\nu_4$	$A_1$	2767.891	2709.708	2710.2099 <sup>g</sup>	2696.656	2695.188	This work
$2\nu_4$	$E$	2801.722	2754.535	2754.7991 <sup>h</sup>	2739.137	2737.466	This work
$\nu_1$	$A_1$	3086.681	3040.513 <sup>e</sup>	3039.49 <sup>f</sup>	3026.139	3024.613	This work

<sup>a</sup> Calculated with the potential from ref. 12 and 16. The MCTDH calculations of ref. 16 gave somewhat different results for the same potential due to neglect of a kinetic energy coupling term as pointed out in ref. 46. Our calculations include all of these terms and should be accurate (for this surface). <sup>b</sup> Calculated with potential from ref. 14. <sup>c</sup> From ref. 47. <sup>d</sup> From ref. 48. <sup>e</sup> Two further levels carry  $\nu_1$ -oscillator strength at  $3022.84\text{ cm}^{-1}$  and  $3030.14\text{ cm}^{-1}$ . <sup>f</sup> Vibrational ( $J = 0$ ) eigenstate estimate from  $P(1)$  line assignment of band I in ref. 10, a second  $P(1)$  assignment (band II in ref. 10) gives a vibrational eigenstate ( $J = 0$ ) at  $3029.00\text{ cm}^{-1}$ . <sup>g</sup> Ref. 4 gave  $2710.210\text{ cm}^{-1}$ . <sup>h</sup> Ref. 49 gave  $2754.796\text{ cm}^{-1}$ .

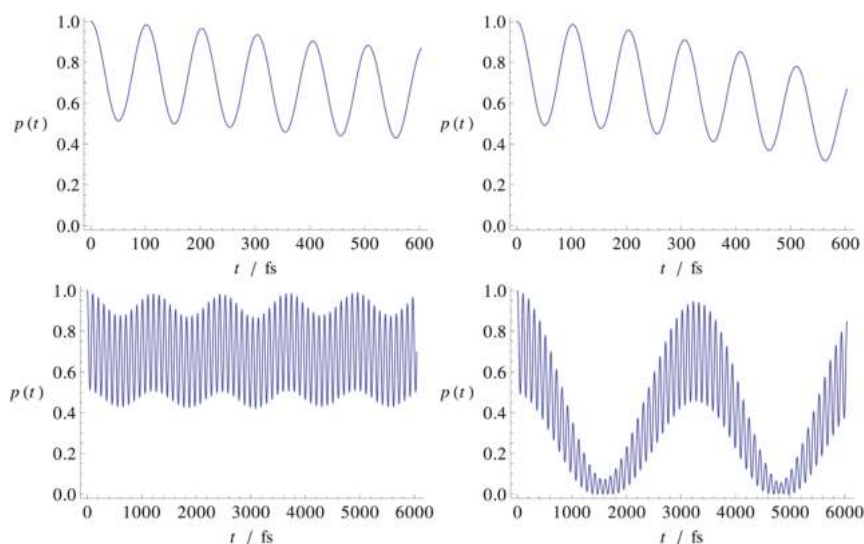


Fig. 4 Survival probability calculated for the CH-chromophore of  $^{13}\text{CHF}_3$  (left) and for  $^{12}\text{CHF}_3$  (right) for time scales of 600 fs (top) and 6000 fs (bottom).

assignments in column 1 of Table 2 have a very approximate meaning serving only for reference to label the eigenstates, which have in fact substantial further contributions from other zero-order states.

We used the calculated vibrational eigenstates (denoted with  $\phi_k(\mathbf{Q})$ ) to expand the time-dependent wavepacket

$$\Psi(\mathbf{Q}, t) = \sum_k c_k(t) \phi_k(\mathbf{Q}), \quad (7)$$

as an exact solution of the time-dependent Schrödinger equation, with the time dependence of the expansion coefficients  $c_k(t) = c_k(0) \cdot \exp(-2\pi i E_k t / \hbar)$ , where initial coefficients  $c_k(0) = \langle \phi_k(\mathbf{Q}) | \Psi(\mathbf{Q}, 0) \rangle_{\mathbf{Q}}$  are obtained by decomposing the initial wavepacket in the basis of the vibrational eigenstates.

The initial state  $\Psi(\mathbf{Q}, 0)$  for investigating IVR dynamics has been chosen to be a product of a Morse oscillator eigenstate (for mode  $\nu_1$  with one quantum,  $\nu_1 = 1$ ) and harmonic oscillator eigenstates (for the remaining modes, all with  $\nu_i = 0$ ). The parameters for defining the effective CH Morse potential were taken from ref. 7.  $\Psi(\mathbf{Q}, 0)$  is meant to model the pure CH stretching as ‘‘chromophore’’ state. For a rough survey of the time-dependent IVR we evaluate the survival probability

$$p(t) = |\langle \Psi(\mathbf{Q}, 0) | \Psi(\mathbf{Q}, t) \rangle|^2, \quad (8)$$

of the initial state  $\Psi(\mathbf{Q}, 0)$ . The  $p(t)$  functions for two different timescales are shown in Fig. 4.

For both isotopomers one can easily identify two main oscillation periods. The short oscillation period is about 100 fs for both

isotopomers with also a similarly large amplitude of the oscillation. This corresponds to the well established CH stretching–bending resonance (exchange of excitation between  $\nu_1$  and  $2\nu_4(A_1)$ ). The second oscillation period is very different both in amplitude and in time for the two isotopomers. For  $^{13}\text{CHF}_3$  the amplitude is small, corresponding to little transfer of excitation to “ $\nu_4 + \nu_5 + \nu_6(A_1)$ ” which can be roughly identified with the eigenstate calculated at  $2999.038\text{ cm}^{-1}$ , resulting in a beating with the state at  $3026.139\text{ cm}^{-1}$  (“ $\nu_1$ ”) and a period of about 1.23 ps. The eigenstate calculated at  $3019.39\text{ cm}^{-1}$  contributes very weakly as well. In contrast, for  $^{12}\text{CHF}_3$  the amplitude is maximal to a complete transfer of excitation from “ $\nu_1$ ” to “ $\nu_4 + \nu_5 + \nu_6(A_1)$ ”, where obviously the eigenstate labeling in terms of zero order states has little meaning. However the beating from the eigenstates calculated as  $3040.51\text{ cm}^{-1}$  (“ $\nu_1$ ”) and  $3030.14\text{ cm}^{-1}$  (“ $\nu_4 + \nu_5 + \nu_6(A_1)$ ”) with a splitting of  $10.37\text{ cm}^{-1}$  results in the visible period of about 3.2 ps. Further, weaker contributions arise from eigenstates at  $3022.84\text{ cm}^{-1}$  (“ $\nu_2 + \nu_4 + \nu_6(A_1)$ ”) and  $2995.49\text{ cm}^{-1}$  (“ $2\nu_5 + \nu_3(A_1)$ ”).

Obviously, while a discussion of times in terms of the eigenstate decomposition in eqn (7) is unambiguous, the discussion in terms of a transfer of excitation between zero order states remains ambiguous and depends on the definition of the basis. Nevertheless, there remains interest in such an approximate description. In the early discussion of the close resonance in ref. 3 several possible candidates were identified to be involved in close anharmonic resonances with  $\nu_1$  (beyond the strong resonance with  $2\nu_4$ ) in  $^{12}\text{CHF}_3$ . Of these, our calculations identify four partners, if one sets an arbitrary threshold at  $10^{-3}$  for the population of the eigenstate in the Morse oscillator initial state and assigns these by their dominant contribution in terms of zero order states ( $\nu_1$ ,  $\nu_4 + \nu_5 + \nu_6$ ,  $\nu_2 + \nu_4 + \nu_6$  and  $\nu_3 + 2\nu_5$ ), all mentioned in ref. 3 already, which also included  $6\nu_6$  and  $2\nu_3 + \nu_5 + \nu_6$  as candidates. Pine *et al.*<sup>10</sup> discussed a preliminary analysis in terms of a model involving  $\nu_1$ ,  $\nu_4 + \nu_5 + \nu_6$ ,  $\nu_2 + \nu_4 + \nu_6$ . Accepting the  $P(1)$  assignments in their spectra for two of the components one obtains the vibrational eigenstates at  $3039.49\text{ cm}^{-1}$  and  $3029.00\text{ cm}^{-1}$ , which agree with the calculated values to within about  $1\text{ cm}^{-1}$ . The splittings defining the longer period, agree within about  $0.1\text{ cm}^{-1}$  between experiment and theory. While a complete analysis of the complex resonance system in  $^{12}\text{CHF}_3$  has defeated several attempts since 1981 in spite of the availability of spectra at low temperatures and in molecular beams,<sup>3,8–10,36</sup> the present conclusions for the time evolution can be considered to be firm, because of the validation of the potential hypersurface with the  $^{13}\text{CHF}_3$  isotopomer, where the spectroscopic analysis is unambiguous. In this sense the dynamics of  $^{13}\text{CHF}_3$  act as a proxy for  $^{12}\text{CHF}_3$ , where uncertainties remain in the CH stretching spectra.

The different time scales for energy flow between stretching and bending within the CH-chromophore (100 fs) and exchange of the energy with the heavy atom frame (11 ps) were discussed from the earliest analyses of the close resonances.<sup>3–7,12–14,16,49–54</sup> The CH stretching–bending system was the first of its kind where the time evolution was discussed with quantum wave packet analyses.<sup>1,5,6</sup> Later, full-dimensional quantum dynamics

were studied on several potential hypersurfaces,<sup>12–16,55</sup> demonstrating the different time scales in qualitative agreement with the earlier estimates.<sup>2–7</sup> Major progress in *ab initio* calculations of potential hypersurfaces for vibrational dynamics,<sup>56–58</sup> as well as full-dimensional vibrational eigenstate calculations on such surfaces<sup>11,59,60</sup> has allowed for the construction of potential hypersurfaces of polyatomic molecules at near to spectroscopic accuracy.<sup>61</sup> In particular, our comparative analysis of the spectroscopy and quantum dynamics of the two isotopomers  $^{12}\text{CHF}_3$  and  $^{13}\text{CHF}_3$  has shown that the potential hypersurface of Ramesh and Sibert III<sup>14</sup> has close to spectroscopic accuracy for trifluoromethane. We thus have now achieved a quantitative understanding of the quantum dynamics for vibrational motion and energy flow in this molecule in the range of the CH stretching fundamental on a time scale from 10 fs to up to 10 ps where both the energy flow between the CH chromophore modes and the flow of energy into the heavy atom frame becomes important. Future work should include a full analysis of the rotation–vibration spectra also in  $^{12}\text{CHF}_3$  in view of understanding the energy flow into rotational motion and the more complex vibrational excitations at even longer times. Here as well the study of isotope effects will provide crucial information on the dynamics.<sup>62</sup>

## Acknowledgements

Our work is supported financially by the Swiss National Science Foundation (SNF), ETH Zürich (in particular the Laboratory of Physical Chemistry) and an ERC Advanced Grant. We are grateful to Professors E. L. Sibert III and H.-D. Meyer, as well as J. Breidung and W. Thiel for useful correspondence and providing PES and DMS source codes and to Carine Manca-Tanner, Roberto Marquardt, Frédéric Merkt, Georg Seyfang, and Jürgen Stohner for discussions. Part of the research was funded from Tomsk Polytechnic University Competitiveness Enhancement program grant, project TPU CEP-PTI-72/2017. We also acknowledge support from COST MOLIM.

## References

- 1 S. Albert, K. Keppler Albert, H. Hollenstein, C. Manca Tanner and M. Quack, *Fundamentals of Rotation-Vibration Spectra*, in *Handbook of High-resolution Spectroscopy*, ed. M. Quack and F. Merkt, Wiley, Chichester, 2011, vol. 1, pp. 117–173.
- 2 M. Quack, *Annu. Rev. Phys. Chem.*, 1990, **41**, 839–874.
- 3 H.-R. Dübal and M. Quack, *Chem. Phys. Lett.*, 1981, **80**, 439–444.
- 4 H.-R. Dübal and M. Quack, *J. Chem. Phys.*, 1984, **81**, 3779–3791.
- 5 R. Marquardt, M. Quack, J. Stohner and E. Sutcliffe, *J. Chem. Soc., Faraday Trans. 2*, 1986, **82**, 1173–1187.
- 6 R. Marquardt and M. Quack, *J. Chem. Phys.*, 1991, **95**, 4854–4876.
- 7 H. Hollenstein, M. Lewerenz and M. Quack, *Chem. Phys. Lett.*, 1990, **165**, 175–183.
- 8 A. Amrein, M. Quack and U. Schmitt, *Mol. Phys.*, 1987, **60**, 237–248.
- 9 A. Amrein, M. Quack and U. Schmitt, *J. Phys. Chem.*, 1988, **92**, 5455–5466.

- 10 A. Pine, G. Fraser and J. Pliva, *J. Chem. Phys.*, 1988, **89**, 2720–2728; A. Pine and J. M. Pliva, *J. Mol. Spectrosc.*, 1988, **130**, 431–444.
- 11 A. G. Császár, C. Fábri, T. Szidarovszky, E. Mátyus, T. Furtenbacher and G. Czako, *Phys. Chem. Chem. Phys.*, 2012, **14**, 1085–1106.
- 12 A. T. Maynard, R. E. Wyatt and C. Iung, *J. Chem. Phys.*, 1995, **103**, 8372–8390.
- 13 A. Maynard, R. E. Wyatt and C. Iung, *J. Chem. Phys.*, 1997, **106**, 9483–9496.
- 14 S. G. Ramesh and E. L. Sibert III, *Mol. Phys.*, 2005, **103**, 149–162.
- 15 J. Breidung, J. Coslou, J. Demaison, K. Sarka and W. Thiel, *Mol. Phys.*, 2004, **102**, 1827–1841.
- 16 L. J. Doriol, F. Gatti, C. Iung and H.-D. Meyer, *J. Chem. Phys.*, 2008, **129**, 224109.
- 17 D. W. Lupo and M. Quack, *Chem. Rev.*, 1987, **87**, 181–216.
- 18 M. Quack, *Infrared Phys.*, 1989, **29**, 441–466.
- 19 M. Quack, *Infrared Phys. Technol.*, 1995, **36**, 365–380.
- 20 R. Widmer, Doctoral Dissertation ETH Nr. 21307, Eidgenössische Technische Hochschule Zürich (ETH Zürich), Zürich, 1989.
- 21 O. V. Boyarkin, M. Kowalczyk and T. R. Rizzo, *J. Chem. Phys.*, 2003, **118**, 93–103.
- 22 R. Bossart, O. V. Boyarkin, A. A. Makarov and T. R. Rizzo, *J. Chem. Phys.*, 2007, **126**, 054302.
- 23 M. Lewerenz and M. Quack, *Chem. Phys. Lett.*, 1986, **123**, 197–202.
- 24 H. R. Dübal, M. Lewerenz and M. Quack, *J. Chem. Phys.*, 1986, **85**, 34–39.
- 25 H. Hollenstein, D. Luckhaus and M. Quack, *J. Mol. Struct.*, 1993, **294**, 65–69.
- 26 D. Romanini and A. Campargue, *Chem. Phys. Lett.*, 1996, **254**, 52–58.
- 27 I. B. Bolotova, Doctoral Dissertation ETH Nr. 24124, Eidgenössische Technische Hochschule Zürich (ETH Zürich), Zürich, 2017.
- 28 I. Bolotova, O. Ulenikov, E. Bekhtereva, S. Albert, Z. Chen, H. Hollenstein, D. Zindel and M. Quack, *J. Mol. Spectrosc.*, 2017, **337**, 96–104.
- 29 L. Andrews, H. Willner and F. T. Prochaska, *J. Fluorine Chem.*, 1979, **13**, 273–278.
- 30 S. Albert, S. Bauerecker, M. Quack and A. Steinlin, *Mol. Phys.*, 2007, **105**, 541–558.
- 31 S. Albert, K. K. Albert and M. Quack, High-Resolution Fourier Transform Infrared Spectroscopy, in *Handbook of High-resolution Spectroscopy*, ed. M. Quack and F. Merkt, Wiley, Chichester, 2011, vol. 2, pp. 965–1019.
- 32 O. Ulenikov, A. Malikova, S. Alanko, M. Koivusaari and R. Anttila, *J. Mol. Spectrosc.*, 1996, **179**, 175–194.
- 33 O. Ulenikov, G. Onopenko, N. Tyabaeva, S. Alanko, M. Koivusaari and R. Anttila, *J. Mol. Spectrosc.*, 1997, **186**, 293–313.
- 34 O. Ulenikov, G. Onopenko, N. Tyabaeva, J. Schroderus and S. Alanko, *J. Mol. Spectrosc.*, 1999, **193**, 249–259.
- 35 O. Ulenikov, E. Bekhtereva, V. Kozinskaia, J.-J. Zheng, S.-G. He, S.-M. Hu, Q.-S. Zhu, C. Leroy and L. Pluchart, *J. Mol. Spectrosc.*, 2002, **215**, 295–308.
- 36 S. Albert, S. Bauerecker, E. Bekhtereva, I. Bolotova, H. Hollenstein, M. Quack and O. Ulenikov, 2017, to be published.
- 37 M. Quack, *Mol. Phys.*, 1977, **34**, 477–504.
- 38 M. Quack, Fundamental Symmetries and Symmetry Violations from High Resolution Spectroscopy, in *Handbook of High-resolution Spectroscopy*, ed. M. Quack and F. Merkt, Wiley, Chichester, 2011, vol. 1, pp. 659–722.
- 39 G. Herzberg, *Molecular spectra and molecular structure. II. Infrared and Raman spectra of polyatomic molecules*, D. Van Nostrand Company, Inc., New York, 1945.
- 40 F. Merkt and M. Quack, Molecular Quantum Mechanics and Molecular Spectra, Molecular Symmetry, and Interaction of Matter with Radiation, in *Handbook of High-resolution Spectroscopy*, ed. M. Quack and F. Merkt, Wiley, Chichester, 2011, vol. 1, pp. 1–55.
- 41 M. J. Frisch, G. W. Trucks, H. B. Schlegel, G. E. Scuseria, M. A. Robb, J. R. Cheeseman, G. Scalmani, V. Barone, G. A. Petersson, H. Nakatsuji, X. Li, M. Caricato, A. Marenich, J. Bloino, B. G. Janesko, R. Gomperts, B. Mennucci, H. P. Hratchian, J. V. Ortiz, A. F. Izmaylov, J. L. Sonnenberg, D. Williams-Young, F. Ding, F. Lipparini, F. Egidi, J. Goings, B. Peng, A. Petrone, T. Henderson, D. Ranasinghe, V. G. Zakrzewski, J. Gao, N. Rega, G. Zheng, W. Liang, M. Hada, M. Ehara, K. Toyota, R. Fukuda, J. Hasegawa, M. Ishida, T. Nakajima, Y. Honda, O. Kitao, H. Nakai, T. Vreven, K. Throssell, J. A. Montgomery, Jr., J. E. Peralta, F. Ogliaro, M. Bearpark, J. J. Heyd, E. Brothers, K. N. Kudin, V. N. Staroverov, T. Keith, R. Kobayashi, J. Normand, K. Raghavachari, A. Rendell, J. C. Burant, S. S. Iyengar, J. Tomasi, M. Cossi, J. M. Millam, M. Klene, C. Adamo, R. Cammi, J. W. Ochterski, R. L. Martin, K. Morokuma, O. Farkas, J. B. Foresman and D. J. Fox, *Gaussian 09, Revision A.02*, Gaussian, Inc., Wallingford, CT, 2016.
- 42 C. A. Burrus and W. Gordy, *J. Chem. Phys.*, 1957, **26**, 391–394.
- 43 M. A. O. Pashaev, O. I. Baskakov, B. I. Polevoy and S. F. Dyubko, *J. Mol. Spectrosc.*, 1988, **131**, 1–8.
- 44 R. Bocquet, D. Boucher, W. Chen, D. Papousek, G. Wlodarczak and J. Demaison, *J. Mol. Spectrosc.*, 1994, **163**, 291–299.
- 45 H. Chambers, R. Kirk, J. Thompson, M. Warner and P. Wilt, *J. Mol. Spectrosc.*, 1975, **58**, 76–86.
- 46 P. Cassam-Chenai, Y. Scribano and J. Liévin, *Chem. Phys. Lett.*, 2008, **466**, 16–20.
- 47 A. Ceausu-Velcescu, J. Cosléou, J. Demaison, G. Graner, G. Duxbury and H. Bürger, *J. Mol. Spectrosc.*, 2003, **220**, 291–297.
- 48 N. J. Fyke, P. Lockett, J. K. Thompson and P. M. Wilt, *J. Mol. Spectrosc.*, 1975, **58**, 87–101.
- 49 J. Segall, R. N. Zare, H. R. Dübal, M. Lewerenz and M. Quack, *J. Chem. Phys.*, 1987, **86**, 634–646.
- 50 O. V. Boyarkin, R. D. F. Settle and T. R. Rizzo, *Ber. Bunsen-Ges. Phys. Chem.*, 1995, **99**, 504–513.
- 51 O. Boyarkin and T. Rizzo, *J. Chem. Phys.*, 1995, **103**, 1985–1988.
- 52 O. V. Boyarkin and T. R. Rizzo, *J. Chem. Phys.*, 1996, **105**, 6285–6292.
- 53 M. Quack, *J. Mol. Struct.*, 1993, **292**, 171–195.
- 54 M. Quack and W. Kutzelnigg, *Ber. Bunsen-Ges. Phys. Chem.*, 1995, **99**, 231–245.

- 55 C. Iung, F. Gatti and H.-D. Meyer, *J. Chem. Phys.*, 2004, **120**, 6992–6998.
- 56 Y. Yamaguchi and H. F. Schaefer III, Analytic Derivative Methods in Molecular Electronic Structure Theory: A New Dimension to Quantum Chemistry and its Applications to Spectroscopy, in *Handbook of High-resolution Spectroscopy*, ed. M. Quack and F. Merkt, Wiley, Chichester, 2011, vol. 1, pp. 325–362.
- 57 D. P. Tew, W. Klopper, R. A. Bachorz and C. Hättig, Ab Initio Theory for Accurate Spectroscopic Constants and Molecular Properties, in *Handbook of High-resolution Spectroscopy*, ed. M. Quack and F. Merkt, Wiley, Chichester, 2011, vol. 1, pp. 363–388.
- 58 J. Breidung and W. Thiel, Prediction of Vibrational Spectra from Ab Initio Theory, in *Handbook of High Resolution Spectroscopy*, ed. M. Quack and F. Merkt, Wiley, Chichester, 2011, vol. 1, pp. 389–403.
- 59 J. Tennyson, High Accuracy Rotation – Vibration Calculations on Small Molecules, in *Handbook of High-resolution Spectroscopy*, ed. M. Quack and F. Merkt, Wiley, Chichester, 2011, vol. 1, pp. 551–571.
- 60 T. Carrington, Using Iterative Methods to Compute Vibrational Spectra, in *Handbook of High-resolution Spectroscopy*, ed. M. Quack and F. Merkt, Wiley, Chichester, 2011, vol. 1, pp. 573–585.
- 61 R. Marquardt and M. Quack, Global Analytical Potential Energy Surfaces for High-resolution Molecular Spectroscopy and Reaction Dynamics, in *Handbook of High-resolution Spectroscopy*, ed. M. Quack and F. Merkt, Wiley, Chichester, 2011, vol. 1, pp. 511–549.
- 62 M. Hippler, E. Miloglyadov, M. Quack and G. Seyfang, Mass and Isotope-Selective Infrared Spectroscopy, in *Handbook of High-resolution Spectroscopy*, ed. M. Quack and F. Merkt, Wiley, Chichester, 2011, vol. 2, pp. 1069–1118.
- 63 O. N. Ulenikov, E. S. Bekhtereva, A. L. Fomchenko, A. G. Litvinovskaya, C. Leroy and M. Quack, *Mol. Phys.*, 2014, **112**, 2529–2556.
- 64 X. G. Wang and T. Carrington, Jr, *J. Chem. Phys.*, 2001, **114**, 1473–1477.